3D effects on transport and plasma control in the TJ-II stellarator

F. Castejón[1] and the TJ-II team[1] and collaborators[2]

[1]Laboratorio Nacional de Fusión, CIEMAT, 28040, Madrid, Spain

[2]Institute of Plasma Physics, NSC KIPT, Ukraine; Institute of Nuclear Fusion, RNC Kurchatov Institute, Moscow, Russia; A.F. Ioffe Physical Technical Institute, St Petersburg, Russia; General Physics Institute, Moscow, Russia; IPFN, Lisbon, Portugal; Kyoto University, Japan; Max-Planck-Institut für Plasmaphysik, Greifswald, Germany; NIFS, Japan; Universidad Carlos III, Madrid, Spain; University of California-San Diego, USA; BIFI, Universidad de Zaragoza, Spain; SWIF, Chengdu, China

E-mail contact of main author: francisco.castejon@ciemat.es

Abstract. The effects of 3D geometry are explored in TJ-II and are two-folded: enhancement of neoclassical transport and modification of stability and dispersion relation of waves. Particle fuelling and impurity transport are studied considering the 3D transport properties. The effect of the 3D magnetic topology on stability, confinement and Alfvén Eigenmodes properties are also explored. Finally, we show here innovative power exhaust scenarios using liquid metals.

1. Introduction

Stellarator devices are well suited to study the relation between 3D magnetic topology, electric fields and transport. This is a relevant topic not only for stellatarors, which are inherently 3D devices, but also for tokamaks, where the axisymmetry can be broken due to the introduction of resonant magnetic perturbations [1] or because of the insert of test blanket modules between the coils (see e. g. [2]). The break of axisymmetry implies the enhancement of neoclassical (NC) transport (see e. g. [3] and references therein), with the subsequent onset of an ambipolar electric field, and the strong modification of the dispersion relation of waves in the plasma in comparison with the axisymmetric case. This paper is devoted to explore the effect of 3D geometry on plasma transport and stability, taking advantage of the TJ-II configuration and flexibility, complemented with the access to results of the new Helias stellarator Wendelstein 7-X (W7-X).

The TJ-II heliac is a four period stellarator with helical magnetic axis and with a bean shaped plasma [4]. Changing the currents that circulate by the coils allows us to modify the magnetic configuration shot to shot or even dynamically in a discharge. Moderated OH and Electron Cyclotron driven currents can be also used to change the rotational transform profile in a discharge. Recent improvements in TJ-II plasma diagnostics, including the operation of a dual Heavy Ion Beam Probe (HIBP), a pellet injection system and liquid Li and LiSn limiters (LLL), have allowed us to get a better understanding of plasma confinement properties. The duplication of the HIBP system enables the measurements in two distant toroidal planes separated by 90^0, opening the exploration of asymmetries in electrostatic potential and the search for long range correlation in relevant plasma magnitudes like electric field [5], which is an indication of the existence of zonal flows (ZFs) [6]. The pellet injector enables the research on core plasma fuelling as well as the exploration of transport and topology properties. The LLL is basic for performing wall coating experiments.

The heating systems for our plasmas consist of two gyrotrons delivering 300 kW each, at X mode with frequencies of 53.2 GHz, i. e., at second harmonic, plus two Neutral Beam Injectors (NBI), which launch co- and counter-beams with 700 kW port-through power at about 33 kV. Although TJ-II plasmas are usually created by Electron Cyclotron Resonance

Heating (ECRH) [7], direct generation of NBI plasmas in TJ-II under lithium coated walls has been obtained without the help of any other external power supply.

The reminder of this paper is organised as follows. Section 2 is devoted to the study of impurity transport, section 3 considers the plasma fuelling properties in TJ-II; section 4 shows the innovative power exhaust scenarios. The stability properties are revised in section 5; section 6 deals with the momentum transport in 3D geometries and section 7 studies the Alfvén mode properties. Conclusions are extracted in section 8.

2. Improving confidence in impurity transport predictions: plasma potential asymmetries and physics of empirical actuators

Impurity accumulation is a key open issue in stellarators and in more general 3D geometries, since the NC transport causes inwards impurity transport in high-density plasmas, because those plasmas are in the neoclassical ion-root. This accumulation would cause strong radiation losses, which would jeopardise the performance of a stellarator fusion reactor. Nevertheless, impurity accumulation is prevented in some experimental cases, namely in the impurity hole regime in LHD [8] and in the HDH mode in Wendelstein 7-AS [9], so the research on these regimes and on the mechanisms for impurity accumulation is mandatory. An intermachine study of impurity transport [10] has been conducted using data from impurity hole LHD plasmas and TJ-II low density NBI scenarios, and documented discharges available at the International Stellarator/Heliotron Database (ISHDB). The goal is to study, with experiments and simulations, the parameter dependence of the thermodynamical forces that drive impurity transport in the low-collisionality regime of a helical device with Ti ≈ Te. These plasmas present small and negative radial electric field, so that the inwards impurity pinch associated to Er is close to be balanced by that related to the temperature gradient, in the outwards direction. As a consequence of this, although there is no temperature screening, the total inwards impurity pinch is relatively small, and this can make it easier for turbulent fluxes or additional neoclassical fluxes associated to asymmetries, as discussed below, to overcome it and reduce the impurity content of the plasma.

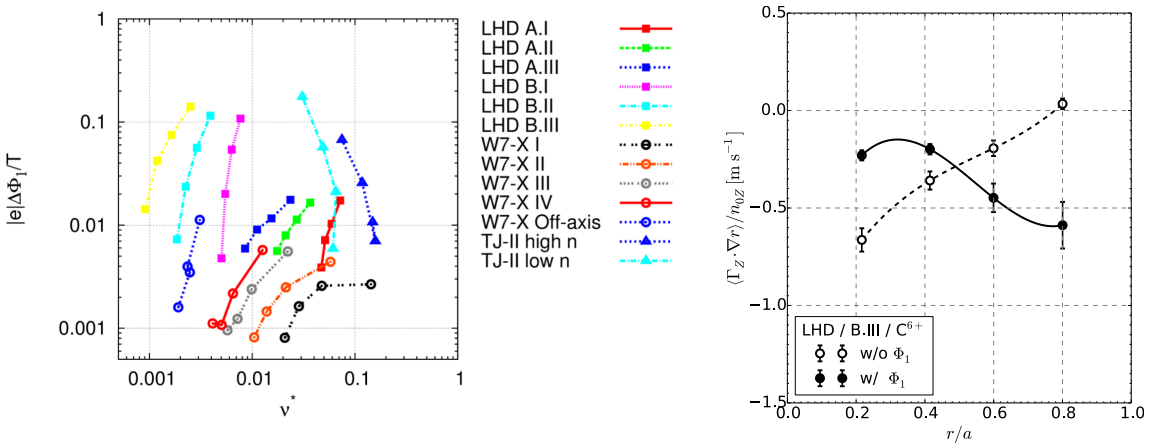

FIGURE 1 (Left) Ratio $e\Delta\Phi_1$ /T as a function of the normalized collision frequency for different positions and profiles sets (each corresponding to a set of points linked by a line). Here e is the unit charge, T the bulk ion temperature and $\Delta\Phi_1$ the maximum potential variation on a surface. (Right) Radial particle flux of C^{6+} in LHD normalized to the density, with and without Φ_1

Three-dimensional NC calculations predict the existence of asymmetries of the neoclassical electric potential on the flux surface, Φ_1, and its impact on impurity transport. Thus, the short length scale turbulent electrostatic potential or its long wave-length variation on the flux surface, Φ_1, usually neglected in the standard neoclassical approach, might shed some light on

the experimental findings. This part of the neoclassical potential introduces trapping and radial transport sources that, despite the weak impact on the bulk plasma species, can affect impurity radial particle transport considerably given the larger charge state of these. In fact, the spectrum of Φ_1, its coupling with the distribution function of the impurities and the resulting transport level is highly sensitive to the parameters considered. A comparison across devices (TJ-II, W7-X and LHD) has been performed for typical plasma parameters for each device [11]. The comparison of Φ_1 in these devices is shown in Fig. 1.left. Further theoretical investigations of the influence of Φ_1 on the radial transport of C^{6+} in LHD, W7-X and TJ-II are shown in Ref. [12]. Impurity flux is strongly modified by Φ_1 in LHD, resulting in mitigated/enhanced accumulation at internal/external radial positions (see Fig. 1.right for a C^{6+} example); for W7-X, on the contrary, Φ_1 is expected to be considerably smaller and the transport of C^{6+} not affected up to an appreciable extent; and in TJ-II the potential shows a moderate impact on impurity transport despite the large amplitude of Φ_1 for the parameters considered. We recognize the need of a more exhaustive scan and search for general scaling dependencies, since the impact of Φ_1 can result in mitigation or enhancement of the inward impurity flow, which is particularly clear in LHD. Regarding TJ-II, Φ_1 is found to be the largest compared to the other devices at similar collisionalities, which supports the suitability of TJ-II for the measurement of Φ_1 and study of its impact on the impurity behaviour. In fact, the study of impurity transport in TJ-II gives asymmetries in the impurity concentration on a magnetic surface [13].

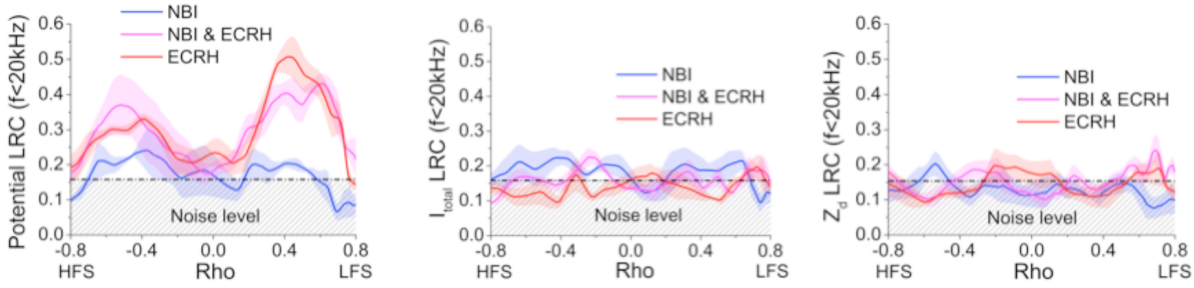

Figure 2. Long Range correlation (LRC) of potential (left), total current, proportional to density (centre), and poloidal magnetic field (right). One of the HIBP systems is fixed at ρ=0.6, while the other is scanned radially.

Experimental studies searching for asymmetries have thrown direct observations of electrostatic potential variations within the same magnetic flux surface [14], allowing the comparisons of impurity density and potential asymmetries with previous models. Significant asymmetries are observed in electron-root wave-heated plasmas, which are reduced in ion-root beam-heated conditions and when the electron temperature decreases. The level of the observed electrostatic potential asymmetries is of tens of volts, which is well reproduced by NC Monte Carlo calculations as it is the dependence of asymmetries on the radial electric field. Significant progress has been made regarding the understanding of empirical actuators, such as ECRH, to avoid core impurity accumulation. The results reported here were obtained using the two HIBP systems, with the unique possibilities of expanding the investigation of multi-scale mechanisms from the plasma edge to the plasma core. Experiments with combined NBI and ECR heating have shown direct experimental evidence of the influence of ECRH on turbulence, increasing both the level of fluctuations and the amplitude of Long-Range-Correlations (LRC), as a proxy of ZFs, for potential fluctuations but not for density and poloidal magnetic fluctuations (see Figure 2), as well as affecting neoclassical radial electric fields. The measurements of Fig. 2 are obtained by fixing one of the HIBP systems at ρ=0.6 and scanning then other one, finding the maximum correlation in potential at that position in ECRH and ECRH+NBI plasmas. Whereas ECRH influences the level of

fluctuations in a wide range of plasma densities, ECRH-induced reversal of the NC radial electric field has been observed only in low-density plasmas [15].

3. Plasma fuelling experiments and neutrals dynamics.

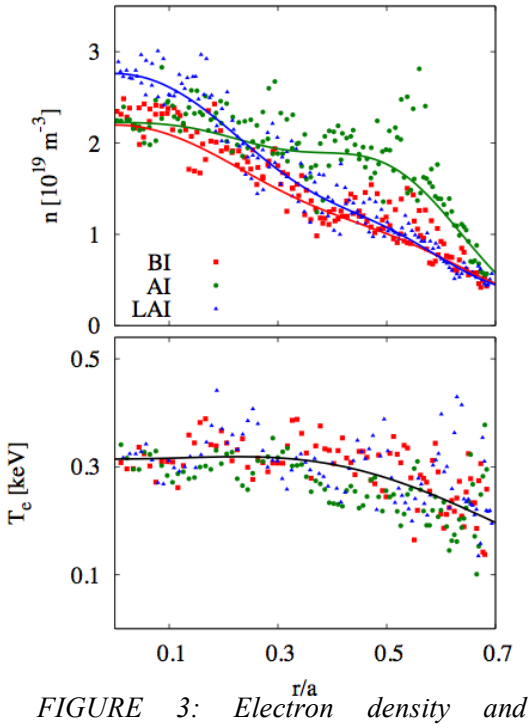

FIGURE 3: Electron density and temperature profiles before the pellet injection (BI, #39063), immediately after the pellet injection (AI, #39062), and long after the pellet injection (LAI, #39065).

Core density control is a critical issue on the path towards the development of steady-state scenarios in 3-D magnetically confined plasmas, especially for the HELIAS line [16]. Therefore, an accurate and precise estimate of core particle transport and core fuelling is of critical interest in order to assess the risk of potential core depletion in large stellarators. This interest has triggered a set of inter-machine comparative pellet fuelling studies [17, 18] whose goal is to achieve a detailed understanding of pellet ablation mechanisms and subsequent particle transport. First core plasma fuelling experiments, using a cryogenic pellet injector system and associated diagnostics have been performed in the TJ-II stellarator [18], which has enabled particle fuelling and transport experiments in this device [19].

We have studied scenarios representative of difficult central fuelling and of loss of density control in NBI plasmas, in which the density (including the core) is reduced by means of gas puff control. A small pellet is injected at an intermediate radial position and density evolution is measured with Thomson Scattering and interferometry. In particular, a density increase due to ablation is initially observed outside the core, moving inwards and reducing with time. Finally, we observe a core density increase after the complete ablation of the pellet, a phenomenon that has been described using NC simulations with DKES code (see Figs. 3 and 4). This phenomenon, if extensible to other helical devices, is of prime relevance: it would mean that pellets that do not reach the magnetic axis may still be able to mitigate core density depletion. Therefore, NC transport is enough to describe transient particle transport after injection of a pellet and, in particular, it predicts indirect core fuelling in scenarios where the pellet ablates outside the core. This is a relevant result in view of density control in reactor-size helical devices, where the penetration depth of the pellet may not be large enough to reach the core for high densities. Pellet injection has been used also to perturb the plasma equilibrium potential and to study the subsequent relaxation. A sudden perturbation of the plasma equilibrium is induced by the injection of a cryogenic hydrogen pellet in the TJ-II stellarator, followed by a damped oscillation in the electrostatic potential, which is observed for the first time [20]. The waveform of the relaxation is consistent with the gyrokinetic

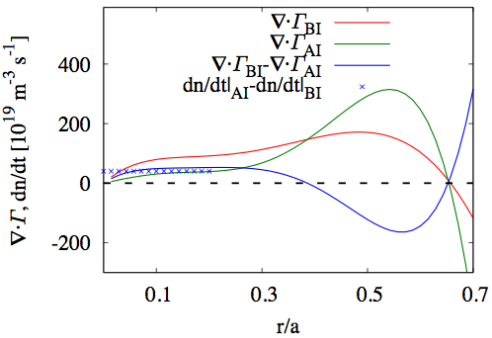

FIGURE 4. Contribution of neoclassical transport, calculated with DKES, to the particle balance equation in NBI plasmas, and comparison with the experiment.

(GK) theory of zonal potential relaxation in a nonaxisymmetric magnetic geometry [21]. The turbulent transport properties of a magnetic confinement configuration are expected to depend on the features of the collisionless damping of ZFs.

Usually, fuelling simulations assume a cloud distribution of neutrals, given by the puffing characteristics. Here, we explore the possible response of neutrals to plasma turbulence, which could modify fuelling properties. With this aim, the helium line-ratio technique was applied with a spectroscopic high-speed camera set-up looking to the emission of helium puffed close to the separatrix. In this way, we obtain the two-dimensional image of the edge plasma electron density with a few millimetres spatial resolution and exposure times down to 15 μ s. This technique allows us to measure the turbulent coherent electron density-structure of blobs that have been compared with the raw helium emission. The differences between plasma density and raw emission structures can give insight on the neutral distribution, provided the rate coefficient for the intensity emission of the lines is known. The conclusion of our measurements point to the fact that the thermal neutrals coming from the puffing valve react to the plasma fluctuations becoming also turbulent at frequencies of 10-100 kHz and with dimensions of one to several centimetres (see Fig. 5). The responsible mechanism to bring neutrals spatially and temporally inhomogeneous would be the turbulent local electron impact ionization by the plasma Blobs and Holes [22]. This can substantially modify the fuelling properties and these results open an almost fully unexplored area of research.

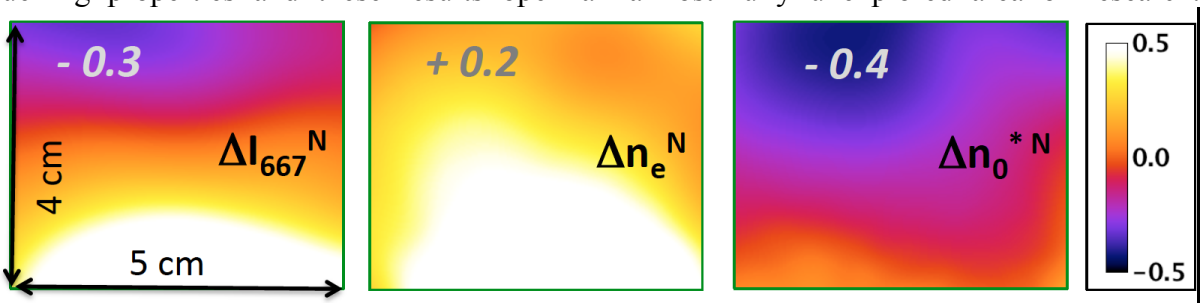

FIGURE 5: From left to right: normalised and de-averaged emission intensity ΔI_{667}^{N}, electron density Δn_e^{N} and neutral density Δn_0^{*N}.

Another key topic for fuelling is whether anomalous transport driven at the plasma edge influences the scrape-off layer (SOL) width. We have performed experiments in the TJ-II Stellarator and have found that the SOL density profile is affected by the structure of edge radial electric fields and fluctuations. It is concluded that SOL profiles are coupled with edge plasma parameters and consequently optimizing SOL power exhaust conditions requires considering transport in the edge region [23].

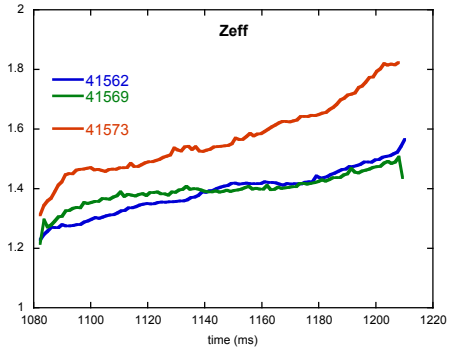

FIGURE 6: Time evolution of Zeff during three reference shots deduced from SXR traces.

4. Innovative power exhaust scenarios using liquid metals.

Novel solutions for plasma facing components based on the use of liquid metals like Li and SnLi alloys have been developed. The TJ-II program on liquid metals, presently leading in the stellarator community, addresses fundamental issues like the tritium inventory control or the self-screening effect of liquid Li driven by evaporation to protect plasma-facing components against huge heat loads, using recently installed Li and SnLi liquid limiters. Biasing of LLL with respect to carbon ones has evidenced the important role of the secondary

electron emission of plasma-exposed surfaces in the development of enhanced confinement modes. Very recently, LiSn alloys have been exposed to TJ-II plasmas in a Capillary Porous System (CPS) arrangement. The evolution of Zeff during the discharge shows that the influx of impurities in the plasma is very small, as can be seen in Figure 6. The main results obtained are [24]:

- H retention values of ~ 0.01% H/(Sn+Li) at T< 450ºC were deduced from Thermal Desorption Spectroscopy (TDS) at the laboratory, in agreement with previous reports and in situ TDS in TJ-II.

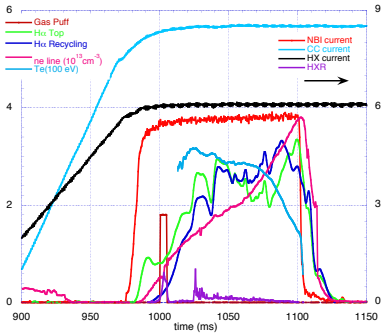

FIGURE 7: Time traces of the NBI start up with full conditioned walls.

- Insertion of a LiSn sample into the edge of TJ-II does not cause any significant perturbation of the plasma parameters. Zeff values typically below 1.5 and very low Prad/Pin values (< 2%) were deduced even with hot samples at the LCFS.
- Conversely, plasma operation became impossible if the alloy is directly deposited on the SS support without mesh.
- Only Li emission was detected. No traces of Sn were detected by visible and UV spectroscopy.
- H recycling did not evolve with temperature.
- Poor thermal conductivity of the CPS of LiSn was deduced for a damaged SS mesh.

These results provide good perspectives for use of LiSn alloys as a PFC in a Reactor.

As a further example of the beneficial effect of Li coating, we achieved plasma start-up in TJ-II under Li-coated walls using only NBI, without the help of any other external power supply, although with large plasma current and high energy electron population. This has been achieved despite the large shine through in the phase of plasma creation [25]. An example of the time traces is shown in Figure 7.

5.- Plasma stability studies.

Experiments on TJ-II have shown that stability at high beta values is better than predicted by linear stability analyses. One of the possibilities offered by TJ-II flexibility is to change the magnetic well keeping the same rotational transform profile. Mercier criterion ensures stable plasmas when the sum of the terms corresponding to magnetic shear, plasma current, geodesic curvature and magnetic well is positive. As the plasma current is negligible and TJ-II is an almost shearless device, the Mercier stability is a play between magnetic well and geodesic curvature. It has been shown that a reduction of magnetic well has a direct impact on fluctuations without reducing plasma confinement [26]. In fact, confinement time depends more on NC effects and on the size of the configuration (see Fig. 8) than on magnetic well. This result shows that Mercier stability calculations are missing some stabilization mechanisms, which could be explained by self-organization processes involving transport and gradients. The effect of the magnetic well scan on electromagnetic modes has also been studied, showing consequences on the onset of a

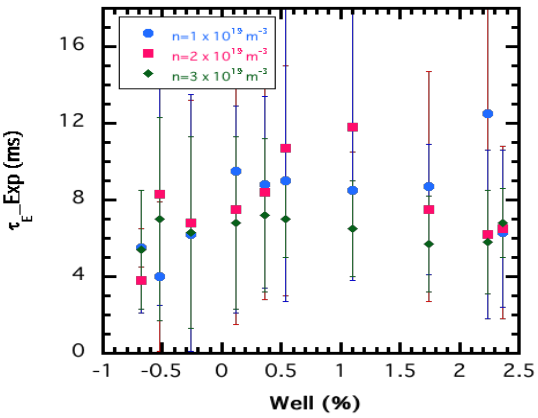

FIGURE 8. Energy confinement times for three values of the plasma density and the values of the magnetic well. Those configurations with negative magnetic value should be unstable.

mode that is a candidate to Geodesic Acoustic Modes (GAMs) and on the Alfvén Eigenmode (AE) properties [27], as will be shown in Section 7.

GAMs are relevant for confinement, given their interaction with broadband turbulence and fast particles, and they are expected to be strongly damped in TJ-II, because of the large ripple and rotational transform values of this device [28]. The latter reason implies that GAMs to survive must be driven steadily to overcome the damping, so a driver must be identified if GAMs are detected. Energetic ions can act as a driver, giving rise to EGAMs [29], which could be the case of Refs. [27, 30]. With confidence, however, fast electrons are acting as a driver for acoustic modes in TJ-II plasmas [31]: experiments have shown intense harmonic oscillations in radiation signals ($\delta I/I \sim 5\%$) during ECRH at low line electron density, $0.15 < ne < 0.6\times10^{19}$ m^{-3}. Their frequency scales with ion sound speed and the poloidal mode structure agrees with that of GAMs, but a $n \neq 0$ toroidal structure is found. The modes are found in the proximity of low-order rationals of the rotational transform ($\iota / 2\pi = 1/q = 8/5$ in these experiments) and are excited by fast-electron populations, but they disappear at the onset of islands rotation. The estimates of correlation between bolometer array signals show a propagation of the mode in the counter-B direction. Figure 9 shows a typical discharge with these excited modes. More work is needed to clarify if we are dealing with EGAMs.

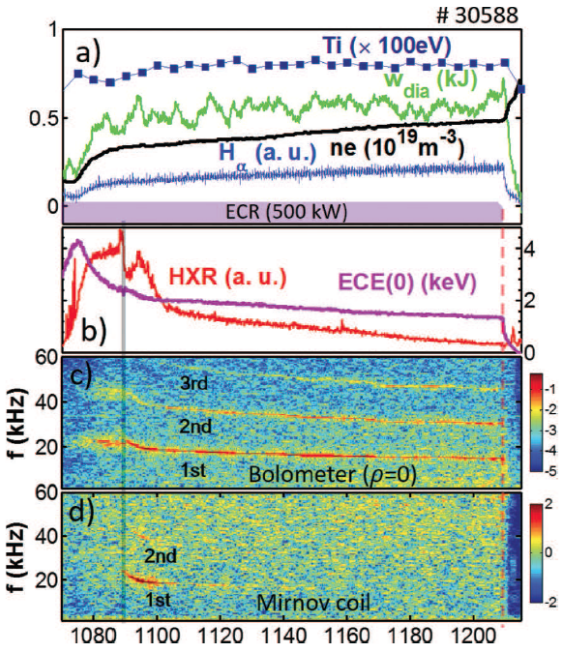

FIGURE 9. Time traces of a discharge with a GAM in TJ-II. Bolometer signal shows the mode all the time, while the magnetic component disappears soon, as measured by Mirnov coils.

The stability of electrostatic modes in TJ-II configurations has been studied by means of global linear GK simulations. Unstable electron-driven modes are found in typical TJ-II plasmas, whose amplitude peaks at very localized spatial regions, determined by both the magnetic field line curvature and the magnetic shear. The high values of the rotational transform tend to the destabilization of electrostatic modes, which is interpreted as a consequence of the mode localization. The effect of strong spatial localization of electrostatic unstable modes has also been studied in non-linear ion temperature gradient (ITG) simulations in TJ-II showing that, although the nonlinear saturation tends to homogenize fluctuations along the flux surface, some signatures of the localization remain both in the fluctuations spectra and bispectra.

6.- Plasma flows and electromagnetic effects.

TJ-II has provided clear evidence of the impact of three-dimensional magnetic structures on plasma confinement and L-H transitions. Observations regarding the temporal ordering of limit cycle oscillations (LCO) at the L-I-H transition, linked to the radial propagation of rotation velocity, emphasize the role of plasma turbulence. LCOs are observed close to the L-H threshold in configurations with a low order rational located inward from the ExB shear location [30]. Furthermore, radial electric fields, ZF-like structures, time memory and radial correlations are modulated by low order rationals [32].

We have also performed experiments on the effect of magnetic islands on the plasma perpendicular flow and density turbulence. Doppler reflectometry have been used to study the plasma flow in Ohmically induced magnetic configuration scans, which changed the rotational transform profile and the location of the rational values of the rotational transform [33]. A characteristic signature of the 3/2 magnetic island as it crosses the Doppler reflectometer measurement position is detected, showing a modulation in the perpendicular flow that changes twice its direction [34]. The perpendicular flow reverses at the centre of the magnetic island and a flow shear develops at the island boundaries. An example is shown in Fig. 10, where the 3/2 magnetic island, in its way from the plasma centre to the plasma edge, crosses the Doppler reflectometer measurement region when the net plasma current is near -5 kA (see Fig. 10 (b) and (c)). Besides, as shown in Fig. 10 (d) and (e), an increase in the perpendicular flow fluctuation intensity is measured at the outer and inner boundaries of the magnetic island; the increase being more pronounced for low frequencies (below 50 kHz). Synchronous with the increase in the flow fluctuations, a reduction in the density fluctuation level is measured (see Fig. 10 (f) and (g)). This reduction is more pronounced in the inner boundary of the island, i.e. when the island is overpassing the Doppler reflectometer measurement region, where the flow shear is stronger. These observations could explain the link between magnetic islands and transport barriers in a number of fusion devices.

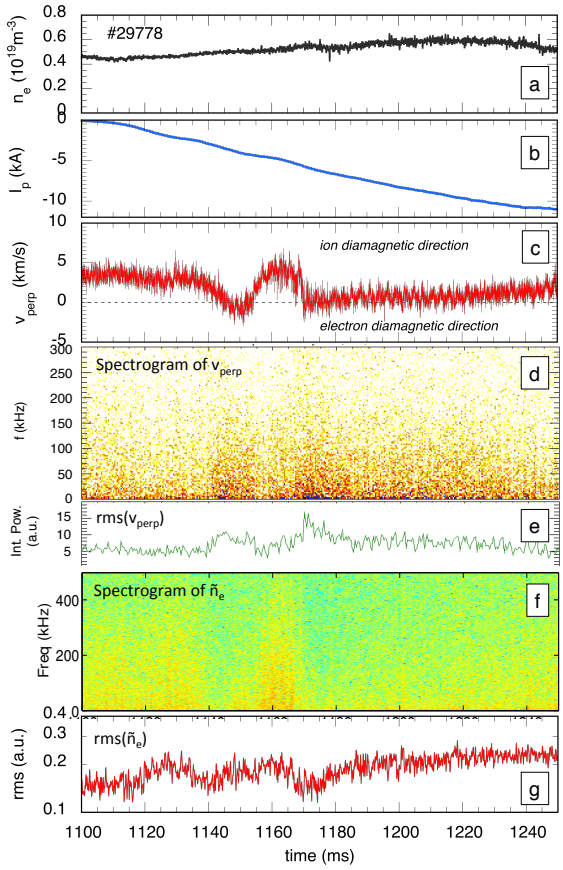

FIGURE 10. The time evolution of line-averaged density (a); net plasma current (b); perpendicular flow (c); spectrogram (d) and root mean square (e) of the perpendicular flow fluctuations, and spectrogram (f) and rms (g) of the density fluctuations.

The relationship between L–H transitions and MHD activity has been also investigated. It is shown that the presence of a low order rational in the plasma edge region lowers the threshold density for H–mode access [35]. MHD activity is systematically suppressed before or at the confinement transition. We apply a novel causality detection technique (the Entropy Transfer) to quantify the information transfer between magnetic oscillations and locally measured plasma rotation velocity related to ZFs and it is confirmed that magnetic oscillations associated with rational surfaces play an important and active role in confinement transitions [36], so that electromagnetic effects should be included in any complete transition of the L-H model. In many cases of L-H transition with co-NB heating and fuelling, we have observed fast repetition rates (~ 1/ms) of transport barrier breaking and re-establishment due to the dynamics of rotating magnetic islands and an enhancement of LRC all the way to the plasma edge. ExB rotation of the islands is compatible with L- and H-confinement modes, while intermediate confinement states characterized by repeated barrier breaking processes seem to imply the rotation of the islands with a diamagnetic drift in the ExB frame [37].

Comparative studies in tokamaks and the TJ-II stellarator [38] in Hydrogen and Deuterium plasmas have shown that there is a systematic increase in the amplitude of LRCs during the transition from H to D dominated plasmas in the tokamaks but not in the TJ-II stellarator, suggesting that ZFs are playing a role on isotopic effect. Furthermore, NC radial electric fields are coupled with the amplitude of LRCs providing evidence of the mutual interaction of NC and turbulent mechanisms in qualitative agreement with GK simulations.

7.- Physics basis for controlling fast particles: the roles of ECRH and magnetic configuration.

The study and control of AEs is basic in plasma devices given the impact of these modes on fast ion confinement, which will influence the fusion performance and the efficiency of heating and current drive. Here we explore several mechanisms to control and mitigate AEs. The HIBP diagnostic is capable to measure simultaneously the oscillations of plasma electric potential, density and poloidal magnetic field, and the Mirnov coils can measure the magnetic fluctuations. The mode position is extracted from the correlation between HIBP signals and Mirnov coils.

First of all, ECRH was applied on NBI-heated low density plasmas of TJ-II. A change from steady to chirping frequency or even to a mitigation of the AEs was observed [39], and the new results show that moderate off-axis ECH power changes the continuous character of the modes significantly, triggering a frequency chirping behaviour. As the ECRH power increases (power scan from 80 to 225 kW), the amplitude of the chirping AE mode increases while the bursts periodicity becomes more regular. A relatively small change of the injection direction of any of the two available ECRH beams modifies the character of the observed AE, from steady to chirping. This change in character is accompanied by a reversal of the plasma current not explained by plasma profile changes. It still remains to clarify if this change in the chirping/steady nature of the AE is due to plasma profile changes or to the modification of damping by ECRH. HIBP measurements show that the chirping mode has a ballooning structure in plasma potential but an anti-ballooning structure in B_{pol}. These experiments show that ECRH is a potential tool for AE control in reactor-relevant conditions.

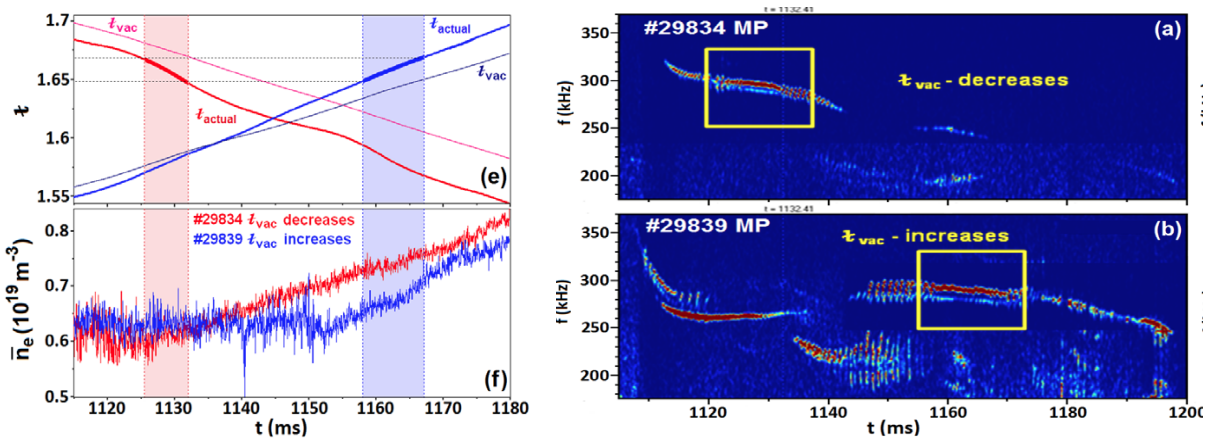

FIGURE 11. Left: time traces of the evolution of the vacuum and actual rotational transform and of the density during the configuration scan. The chirping appears always for the same values of rotational transform (marked with stripes), as can be seen on the right panel. The boxes correspond to the times of the right panel.

On top of the effect of ECRH, we expect the magnetic configuration to have strong effect on AEs properties, since the dispersion relation can be modified varying the configuration. We take advantage of the above-referred TJ-II flexibility to explore the effect of the magnetic configuration on AEs, which opens new ways to control such modes and, hence, their effect

on fast ion confinement. We have introduced OH-induced current in order to vary the rotational transform in TJ-II in a single configuration, which modified strongly the mode properties due to both the change of the wave vector of the mode [40] and the dispersion relation in the plasma. Using the dependence of the parallel wave vector on the mode order and rotational transform value, $k_{\|} \propto \left| n - \frac{m\iota}{2\pi} \right|$, we could identify the mode order.

New experiments consisted on dynamic configuration scans in TJ-II in single discharges. In this way we can explore the change of character of the mode. We used L-mode hydrogen plasmas heated with co-, counter- and balanced NBI and ECRH in various magnetic configurations with rotational transform $\iota(a)/2\pi = 1/q \sim 1.5$ - 1.6. We could observe chirping modes obtained with NBI only in plasmas (without the intervention of ECRH) with densities similar to those of earlier studies (see Figure 11). The absence of ECRH in the discharges studied here shows that this is not a necessary ingredient to obtain chirping modes in TJ-II. Using the HIBP we deduce that the location of the AE chirping mode is between $-0.8 < \rho < 0.8$ in these experiments. Chirping modes have a specific spatial structure: the electric potential perturbations have a ballooning character, while the density and B_{pol} perturbations are nearly symmetric for both ECRH+NBI and NBI-only plasmas. On TJ-II, a dominant effect on the non-linear evolution of the AE from chirping to steady frequency state is the magnetic configuration, determined by vacuum ι and plasma current I_{pl} [41].

The importance of distinguishing chirping from steady behaviour relies on the different effect of the mode on fast ion confinement. We use the fast neutrals flux, measured by the Compact Neutral Particle Analyser (CNPA), as a proxy for the fast ion density, so the larger the CNPA flux the larger the fast ion concentration. Hence, we can compare the fast ion confinement of different experiments by comparing the CNPA spectra, in case that the fast ion source is the same. It is seen that the confinement is better in the cases with chirping and mitigated AE than in the one with steady AE [42].

We have also investigated the influence of magnetic well on AEs properties, taking advantage of the TJ-II flexibility. We have found a strong influence of this parameter on AEs on both, frequency, mode number and amplitude of the mode [27]. The complexity of dispersion relation in TJ-II provokes such a strong change in the mode properties. In particular, it is observed that the frequency of the destabilised modes is decreasing with the magnetic well: the lower the magnetic well the lower the frequency, for similar plasma densities. This allows one to change the population of resonant ions, since one expects that the energy of the resonant ions is lower in the case of lower AE frequencies. The amplitudes of the modes are found to be non-monotonic with the well and the nature and order of the modes change from one configuration to another, since the gaps appear at different frequencies and positions. Global and Helical AEs (GAEs and HAEs) appear in the deep well configurations and only HAEs happen in the hill cases.

AEs studies are commonly based on the basis of equilibrium nested flux surfaces. Nevertheless, magnetic islands can appear close to the rational values of the rotational transform that can modify the AE spectrum and open new gaps in the continuum. In TJ-II, coherent modes in NBI-heated plasmas at frequencies generally below those of helicity induced AEs ($f < f_{HAE}$) are explained as GAEs and discrete shear-AEs induced by a non-rotating magnetic island (MIAE). Rotating islands are also found to interact with AEs: if they share the same helicity, they perturb each other; otherwise, new AEs are excited via wave-wave coupling [43].

8.- Conclusions.

The influence of 3D geometry on confinement physics has been explored taking advantage of

the TJ-II characteristics and advanced diagnostics capability. Access to W7-X results complements these studies. The break of axisymmetry causes that NC transport is not automatically ambipolar, giving rise to the onset of a radial electric field, which has strong influence on particle transport and fuelling. Impurity transport is also affected and we have explored here the conditions in which the inwards impurity pinch is decreased and allow that other transport terms can decrease impurity accumulation. The first order NC theory predicts the existence of asymmetries on the magnetic surfaces, which have been observed experimentally in TJ-II, and can have strong influence on impurity transport.

Experimental observations and NC calculations show central plasma density depletion in low collisionality plasmas, which is a problem detected in helical devices. We have shown that this can be overcome by injecting a pellet, even it is ablated before reaching the plasma centre. Pellet injection has not been only used as fuelling tool, but it has allowed us to obtain for the first time a direct observation of the electric field relaxation, in agreement with GK simulations. Another important characteristic of the fuelling in TJ-II is the structure of the neutrals that reflect the blobs that are found in density turbulence. The coupling of the edge plasma parameters with SOL density profiles has also influence on fuelling, as has been explored here. As the fuelling experiments demonstrate, the plasma wall interaction in TJ-II depends strongly on the 3D geometry and makes TJ-II a well-suited laboratory to explore innovative solutions for plasma facing components based on the use of liquid metals like Li and SnLi alloys.

The 3D geometry has also strong effects on plasma stability and turbulence, since the dispersion relation of the waves and the MHD properties will change strongly with the geometry. We have obtained stable plasmas in theoretically Mercier-unstable configurations and have found that the confinement depends rather on NC properties and volume than on Mercier criterion. Firm candidates to EGAMs driven by fast ions and fast electrons are also detected in TJ-II, showing the effect of rational values of the rotational transform on the latter modes, observed for the first time.

MHD stability and the magnetic island onset have strong influence on momentum transport and on L-H transition. The plasma flow is affected by the magnetic island, as can be directly measured by Doppler reflectometry. The rational values of the rotational transform can give rise to the cyclic formation and destruction of transport barriers, playing a key role in the L-H transitions.

The dispersion relation of AEs is also affected by the 3D geometry. In particular, we have shown that the magnetic well is a governing parameter of the frequency of the mode: the larger the well, the higher the frequency, for the same density. The rotational transform plays a key role in the AEs properties: we have found the rotational transform windows in which the mode presents a chirping nature and the ones in which its frequency varies steadily following plasma current and density. The rational values of the rotational transform can give rise to the presence of islands that trigger MIAEs. This poses the magnetic configuration as another important tool for controlling AEs and, hence, fast ion confinement, beyond ECRH. New experiments show that the amplitude of the chirping AE mode increases while the bursts periodicity becomes more regular, as the ECRH power increases.

Acknowledgements

This work has been carried out within the framework of the EUROfusion Consortium and has received funding from the Euratom research and training programme 2014-2018 under grant agreement No 633053. The views and opinions expressed herein do not necessarily reflect those of the European Comission. This work has been also funded by the Spanish Ministerio de Economía y Competitividad under Projects ENE2013-48109-P, ENE2013-48679-R,

ENE2014-52174-P, ENE2014-58918-R, ENE2014-56517-R, ENE2014-56517-R, ENE2015-64914-C3-1-R, ENE2015-70142-P

[1] T.E. Evans et al. Phys. Rev. Lett. 92 (2004) 235003
[2] A. Bustos et al. Nuclear Fusion 50 (2010) 125007
[3] I. Calvo et al. Plasma Phys. Control. Fusion 55 (2013) 125014
[4] C. Alejaldre et al. Nucl. Fusion 41(2001) 1449
[5] M. A. Pedrosa et al. Phys. Rev. Lett. 100 (2008) 215003
[6] E. Sánchez et al. Plasma Phys. Control. Fusion 55 (2013) 014015
[7] A. Cappa et al. Nucl. Fusion 55 (2015) 043018
[8] M. Yoshinuma et al. Nucl. Fusion 49 062002 (2009)
[9] K. McCormick et al. Physical Review Letters 89 (2002) 015001
[10] J.L. Velasco *et al.,* "Moderation of neoclassical impurity accumulation in high temperature plasmas of helical devices", Nucl. Fusion, submitted (2016)
[11] J. M. García-Regaña et al. Plasma Physics and Controlled Fusion 55 (2013) 074008
[12] J. M. García-Regaña et al. "Electrostatic potential variation on the flux surface and its impact on impurity transport". Submitted. http://arxiv.org/abs/1501.03967
[13] J. A. Alonso et al. Plasma Phys. Control. Fusion 58 (2016) 074009
[14] M. A. Pedrosa et al., Nuclear Fusion 55 (2015) 052001
[15] C. Hidalgo et al. "On the influence of ECRH on neoclassical and anomalous mechanisms using a dual Heavy Ion Beam Probe diagnostic in the TJ-II stellarator", Proc. of 26th IAEA-FEC Conference, EXC/P7-209, Kyoto, Japan, 2016
[16] H. Maassberg et al. Plasma Phys. Control. Fusion 41(1999) 1135
[17] A. Dinklage et al. "The effect of transient density profile shaping on transport in large stellarators and heliotrons", Proc. of 26th IAEA-FEC Conference, EX/P7-47, Kyoto, Japan, 2016
[18] K. McCarthy et al. "Plasma core fuelling by cryogenic pellet injection in the TJ-II stellarator", Proc. of 26th IAEA-FEC Conference, EX/P7-47, Kyoto, Japan, 2016
[19] J.L. Velasco et al., Plasma Phys. Control. Fusion 58 (2016) 084004
[20] A. Alonso et al. "Observation of oscillatory radial electric field relaxation in a helical plasma". Submitted to Physical Review Letters, 2016 (http://arxiv.org/abs/1609.00281)
[21] P. Monreal et al. Plasma Phys. Control. Fusion 58 (2016) 045018
[22] E. de la Cal and the TJ-II Team. Nucl. Fusion 56 (2016) 106031
[23] T. Wu. "Coupling of SOL density profiles with edge plasma parameters in the TJ-II stellarator". Submitted to Nuclear Fusion, 2016
[24] F. L. Tabarés et al. "Experimental tests of LiSn alloys as potential liquid metal for the Divertor target in a Fusion Reactor". 22 PSI Rome 2016. NM&E, in press
[25] F.L. Tabarés et al. "Direct generation of NBI plasmas in TJ-II with lithium coated walls". Stell. News 144
[26] A. M. de Aguilera et al, Nucl. Fusion 55 (2015) 113014
[27] F. Castejón et al. Plasma Phys. Control. Fusion 58 (2016) 094001
[28] E. Sánchez et al. Plasma Phys. Control. Fusion. 55 (2013) 014015
[29] R. Nazikian et al. Physical Review Letters 101 (2008) 185001
[30] T. Estrada et al., Nuclear Fusion 55 (2015) 063005
[31] B.J. Sun, M. A. Ochando, D. López-Bruna. European Physics Letters 115 (2016) 35001
[32] B. van Milligen et al., Nuclear Fusion 56 (2016) 016013
[33] T. Estrada et al. Nuclear Fusion 56 (2016) 026001
[34] T. Estrada et al., "Plasma Flow, Turbulence and Magnetic Islands in TJ-II". Proc of the 26th IAEA-FEC Conference, EXC/P7-45, Kyoto, Japan, 2016
[35] D. López-Bruna et al. Plasma Physics and Controlled Fusion 55 (2013) 015001
[36] B. van Milligen et al. "The causal impact of magnetic fluctuations in slow and fast L-H transitions at TJ-II". Submitted to Nulcear fusion, 2016
[37] D. López-Bruna et al. "Confinement modes and magnetic-island driven modes in the TJ-II stellarator" Proc of the 26th IAEA-FEC Conference. EX/P7-48. Kyoto, Japan, 2016
[38] B. Liu et al. Nuclear Fusion 55 (2015) 112002
[39] K. Nagaoka et al. Nuclear Fusion 53 (2013) 072004
[40] A. Melnikov et al. Nucl. Fusion 54 (2014) 123002
[41] A. Melnikov et al. Nucl. Fusion 56 (2016) 076001
[42] J. M. Fontdecaba et al. "Influence of Alfvén waves on fast ion confinement in TJ-II plasmas". In preparation
[43] B.J. Sun et al., Nuclear Fusion 55 (2015) 093023